

BIOCHE 01425

## Subsidiary hydrogen bonding of intercalated anthraquinonic anticancer drugs to DNA phosphate

Walter Pohle <sup>a</sup>, Martin Bohl <sup>a</sup>, Joachim Flemming <sup>a</sup> and Heinz Böhlig <sup>b</sup>

<sup>a</sup> Central Institute of Microbiology and Experimental Therapy, Academy of Sciences of the G.D.R., Jena and <sup>b</sup> Department of Chemistry, Karl Marx University, Leipzig, G.D.R.

Received 20 April 1989

Accepted 25 July 1989

DNA; Anthraquinone complex; Hydrogen bonding; Infrared spectroscopy; CNDO/2 calculation; Normal coordinate analysis; Anthracycline; Mitoxantrone

Several anthraquinone derivatives are active against different kinds of human cancer. The cancerostatic activity has been mainly attributed to their ability to bind strongly to DNA by intercalation. Here, infrared spectroscopy was used to detect further, more specific DNA interactions with the prominent anticancer drugs daunomycin, adriamycin, aclacinomycin A and mitoxantrone as well as with the cytotoxic violamycin BI. The most striking result was a significant decrease in wave number of the band arising from antisymmetric stretching vibration of the  $\text{PO}_2^-$  groups of DNA upon complexation with adriamycin, aclacinomycin A, violamycin BI and mitoxantrone. This became evident after separation of the contributions from conformational changes of DNA to the influence on the wave number of that band. The drug-induced shift was interpreted in terms of the formation of a hydrogen bond between the intercalated drug molecules and the  $\text{PO}_2^-$  moiety of DNA via the following terminal hydroxyl groups: C14-OH for adriamycin, C4-OH for both aclacinomycin A and violamycin BI and, more tentatively, the external side-chain OH of mitoxantrone. Theoretical considerations, consisting of semi-empirical CNDO/2 calculations as well as normal coordinate analyses performed with molecular model fragments, provided results confirming and rationalising the experimental findings. The capacities of the anthracyclines for restriction of the conformational flexibility of DNA differ, presumably due to variations in the spatial dimensions of the sugar moieties of the drugs. The compatibility of the present results with data obtained from current geometrical models, especially those for the DNA-daunomycin and DNA-adriamycin complexes, is discussed in detail.

### 1. Introduction

Anthraquinones represent a class of substances displaying a large variety of biological effects. Several of the anthraquinone derivatives exhibit distinct antineoplastic activity and a number are now in clinical use. The most prominent agents among the first generation of these drugs are the anthracycline antibiotics daunomycin or daunorubicin (DAM) and adriamycin or doxorubicin (ADM) [1]. Both are active against leukemia, but

ADM is also effective against particular solid tumors and has been regarded for some time as being the most potent antitumor drug known [1]. A disadvantage of both chemicals is that they exert strong side effects, especially cardiotoxicity. This was considered reason enough to undertake an intensive search for new substances with comparable activity but diminished toxicity. Two outstanding developments in this direction are the antibiotic, aclacinomycin A or aclarubicin (ACM), an anthracycline of the second generation [2,3], and the synthetic dihydroxyanthraquinone, mitoxantrone (MX) [4,5].

The mechanism of antineoplastic action of these drugs is most probably rather complex and the

Correspondence address: W. Pohle, Central Institute of Microbiology and Experimental Therapy, Academy of Sciences of the G.D.R., Beutenbergstrasse 11, DDR-6900 Jena, G.D.R.

details remain thus far unknown, but DNA is generally accepted as playing a key role, since considerable interference with its synthesis and functioning occurs upon drug binding [6]. The fundamental mode of binding is unambiguously the intercalation of ligand chromophores between the base-pairs of DNA. Moreover, drug molecules become anchored via relevant substituents to suitable DNA sites by specific subsidiary binding. The problem as to which particular drug substituents are relevant and the pertinent DNA-binding sites involved remains to be resolved. Widely differing opinions, e.g., concerning the closely related DNA-DAM and DNA-ADM complexes, have been expressed [7–11]. For ACM and

MX, there is at present no clear information available on subsidiary drug binding to DNA.

Among the physico-chemical methods employed in studying DNA complexes (a survey referring to DNA-anthracene interactions is given in ref. 12), infrared spectroscopy is a very promising approach to discrimination of sites involved in DNA-drug interactions, since it allows their direct identification [13]. Therefore, we have made intensive use of this procedure to carry out the systematic investigation of complexes formed between DNA and the anthraquinone derivatives ADM, DAM, ACM, MX, and violamycin BI. The structures of the ligands are shown in fig. 1. Infrared spectroscopic measurements also included

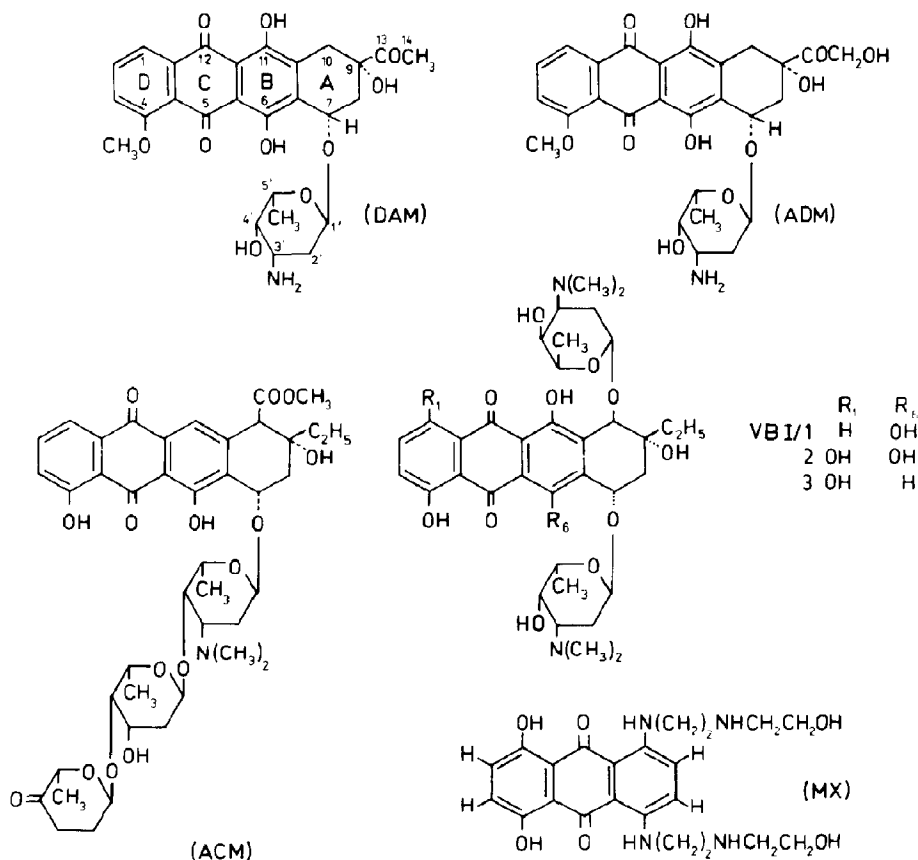


Fig. 1. Structures of the anthraquinone derivatives daunomycin (DAM), adriamycin (ADM), violamycin BI (VBI), aclacinomycin A (ACM) and mitoxantrone (MX).

linear dichroism (LD) in order to obtain more detailed information on the constituents of the complexes and, in particular, on the conformation of DNA. Violamycin BI (VBI) is also an anthracycline antibiotic isolated from fermentation cultures of *Streptomyces violaceus* [14]. It differs from the other members of this class in not being used clinically; it displays a broad spectrum of biological activity (see ref. 15 and papers cited therein). From a heuristic viewpoint, it would be of interest to compare VBI with the other compounds, since its major components contain two amino-sugars attached to ring A at different positions (fig. 1). For investigation of DNA-VBI complexes [16], infrared spectroscopy and X-ray diffraction analysis have been shown to be complementary on combined use [17].

The aim of the present paper is to report and to discuss the principal effects observed for the band ascribed to antisymmetric stretching vibration of the  $\text{PO}_2^-$  moiety of DNA upon complexation. A preliminary account of the results obtained with DAM and ADM has been published [18]. The wave number of the above-mentioned band,  $\tilde{\nu}_a$ , is well known to provide a very sensitive indication of the influence of the environment on the phosphate groups, for instance, upon hydration [19,20]. The experimental data are supplemented by results of quantum-chemical and normal-coordinate calculations using appropriate molecular fragments to model DNA-anthraquinone interactions.

## 2. Materials and methods

### 2.1. Infrared spectroscopy

High-molecular-weight DNA (from salmon sperm; Sigma, U.S.A.; with 0.6% protein) containing an additional amount of NaCl (3–5% w/w) was used to prepare oriented films by unidirectional stroking. Before complexation, samples were studied by infrared spectroscopy on passing through dehydration-rehydration cycles. The relative humidity (R.H.) of the surroundings was adjusted in the infrared cells by means of saturated solutions of appropriate salts and varied between 98 and 23%. The reversible B-A conformational

transition, which was first observed using fiber X-ray diffraction [21] and can be monitored reliably by LD [22,23], occurs at about 86% R.H.

The DNA-anthraquinone complexes cannot be prepared, in general, by direct mixing of the constituents, since the adducts precipitate and are thus unsuitable for orientation. Therefore, drug doses were applied to pre-oriented DNA films from an ethanolic solution as described elsewhere [24]. After evaporation of the ethanol, infrared spectroscopic measurements could be performed as for pure DNA. All the drugs except for VBI (see above) were commercial products (ADM and DAM, Farmitalia, Italy; ACM, Sanraku, Japan; MX, Cyanamide, U.K.), and were used in the form of the hydrochloride without further purification. Their infrared spectra were recorded in KBr discs for comparison with difference spectra obtained by subtraction of the pertinent DNA spectra from those of the complexes.

A computer-coupled Perkin-Elmer model 325 spectrophotometer equipped with a wire-grid polariser on an AgBr support was employed in the infrared spectroscopic investigations. Polarised spectra were analysed by using the algorithm developed by Fraser [25]. All other experimental details were the same as reported in previous articles [17,23,26].

### 2.2. Theoretical calculations

For DNA and DNA-anthraquinone systems, the model fragments illustrated in fig. 8 were investigated by performing semi-empirical CNDO/2 molecular orbital calculations using an SPD basis set and original parametrization [27,28]. The internal coordinates for B-DNA provided by Arnott et al. [29] and from crystallographic data on carminomycin [30] were employed to construct the geometry of the DNA and drug fragments, respectively. In the process of geometry optimization, the following internal coordinates were included: both  $\text{P}=\text{O}$  bond lengths, the  $\text{O}=\text{P}=\text{O}$  bond angle, and the  $\text{O}\cdots\text{H}$  and  $\text{O}-\text{H}$  bond distances. Hydrogen bonding minima refer to CNDO/2-optimised  $\text{H}-\text{O}$  (drug) and  $\text{H}\cdots\text{O}$  (DNA) bond distances of about 107–111 and 122–130 pm, respectively.

Table 1

Conformational flexibility of DNA expressed by  $x_A$ , the fraction of A form in a sample consisting of coexisting A- and B-type structures ( $x_i$ : fraction of DNA where the conformational B-A transition is inhibited), and wave numbers of the band due to antisymmetric stretching vibration of the  $\text{PO}_2^-$  groups of DNA in anthraquinone complexes at different binding ratios,  $r_i$ , and relative humidities surrounding the films;  $n$ , number of independent measurements during dehydration-rehydration cycles;  $\bar{\nu}_a$  values for ACM at  $r_i = 0.04$  and  $0.08$  refer to different samples. The error in  $\bar{\nu}_a$  amounts to  $0.5\text{--}1\text{ cm}^{-1}$ .

Drug	$r_i$	Relative humidity range (%)	$x_A$ (%)	$x_i$ (%)	$\bar{\nu}_a$ (cm <sup>-1</sup> )	$n$
Adriamycin	0	98	10 ± 6		1221	2
		23–76	92 ± 2	8 ± 2	1235	5
	0.04	88–98	0		1218	3
		59–76	34 ± 4	66 ± 4	1222	3
	0.08	23–76	0	100	1215.5	9
Daunomycin	0	98	10 ± 5		1220	2
		59–76	91 ± 5	9 ± 5	1233.5	4
	0.04	88–98	0		1219	4
		59–76	26 ± 3	74 ± 3	1220.5	4
	0.08	23–98	0	100	1220.5	7
Aclacinomycin A	0	98	~ 0		1220	1
		76	95	5	1235	2
	0.04	98	~ 0		1216	2
		59–76	53 ± 4	47 ± 4	1225	4
	0.08	98	0	100	1216	2
		76–88	81 ± 8	19 ± 8	1217	4
	Violamycin BI	0	98	10		1221
59–84			88 ± 3	12 ± 3	1235	2
0.06		98	10		1219	2
		23–84	36 ± 4	64 ± 4	1223	3
0.13		98	~ 0		1218	2
		59–76	34 ± 3	66 ± 3	1220	3
Mitoxantrone		0	98	5 ± 3		1221
	59–76		100	0	1236.5	3
	0.03	98	0		1219	3
		59–76	35	65	1222	3
	0.06	98	0		1217.5	2
		59	27 ± 2	73 ± 2	1222.5	2

In the normal coordinate analysis, the solution of the inverse eigenvalue problem was performed according to the program of Jones [31] which is based on the *GF* matrix formalism of Wilson [32]. The *G* matrices are formed by 20 internal coordinates of the  $\text{O}_2\text{P}(\text{OC})_2$  model, i.e., six stretching, eight bending and six torsional coordinates. Calculations were carried out on the basis of all these internal coordinates. For the *F* matrices, the Urey-Bradley force field (UBFF) for the DNA backbone proposed by Lu et al. [33] was applied with an additional force constant for torsional

motions amounting to  $f = 0.093\text{ N am}$ . The wave number,  $\bar{\nu}_a$ , was evaluated as a function of both the  $\text{P}=\text{O}$  stretching force constant and the  $\text{O}=\text{P}=\text{O}$  valence angle. Variations in these DNA parameters should mimic the influence exerted by hydrogen-bonded drugs.

### 3. Results and discussion

One of the most important observations during analysis of the infrared spectra is that  $\bar{\nu}_a$ , the wave

number of the band arising from antisymmetric stretching vibration of the  $\text{PO}_2^-$  groups of DNA, undergoes drastic change upon varying the experimental conditions (by contrast, the displacements of  $\tilde{\nu}_s$ , the corresponding parameter for symmetric stretching, are very small). The data listed in table 1 provide a representative overview of the systems studied; they reveal dependence of  $\tilde{\nu}_a$  on different parameters: most drastically on relative humidity but more importantly also on the type of drug complexed with DNA and lastly on its relative concentration described by  $r_i$ , the binding ratio of drug molecules per DNA nucleotide. To enable us to differentiate and to understand the drug-induced alterations of  $\tilde{\nu}_a$ , it is necessary to separate the dependence of  $\tilde{\nu}_a$  on relative humidity, or what is closely related to that, on DNA conformation; therefore, the conformational behavior of DNA in the complexes will be considered first. The pertinent data have appeared in abstract form in a preceding paper [34].

### 3.1. Infrared spectroscopic data on DNA conformation in the complexes

Depending on the sequence and environmental conditions prevailing, DNA may adopt various conformations among those belonging to the  $\bar{A}$ ,  $\bar{B}$  and  $\bar{Z}$  families of forms [35]. In samples of native DNA possessing a random sequence, the B and A forms were observed to predominate under conditions of high and medium water activity, respectively [21]. In contrast to X-ray diffraction analysis, infrared spectroscopy can furnish quantitative data on the relative proportions of each conformational type of DNA present in co-existing fractions of the A and B forms [17]. With the aid of particular parameters characteristic of the infrared spectra (two absorption bands specific to the A form and the angle of the transition moment,  $\theta_{\text{OPQ}}$ , determined from linear dichroism of the  $\nu_s(\text{PO}_2^-)$  band), the parameter designated as  $x_A$  may be estimated and hence yield the fraction of A-DNA present in a sample which may also contain B-DNA as a constituent [36]. The value of  $x_A$  under conditions of medium relative humidity in which pure DNA usually occurs in the A form can be taken as a measure of the conformational flexi-

bility of DNA in a given sample and in the complexes. The magnitude of the term  $x_i$  ( $x_i = 1 - x_A$ ) then represents the fraction of DNA on which constraints on the conformation are in existence [37]. The values of both parameters are listed in table 1 for DNA contained in several complexes.

As can be seen, the  $x_A$  values determined for uncomplexed DNA films under conditions of both very high and moderate relative humidity are mostly not strictly equal to zero or unity, i.e., in the films under the given conditions, infrared spectroscopy is generally sufficiently sensitive to demonstrate that the DNA does not occur solely as a single form, and that, in most cases, a small proportion (<12%) of the minor component is present in the major constituent. Contrary to expectation for the particular level of water activity in samples, even larger proportions have been reported, as discussed in ref. 38 for A-DNA in B-type samples and, vice versa, in ref. 39 for B-DNA in A-type samples.

Under conditions of high relative humidity, on ligand addition, the residual content of A-form begins to diminish at low  $r_i$  values and DNA adopts exclusively the B conformation. This trend in behavior is more clearly evident at moderate values of the relative humidity: according to the ratio for drug binding and ligand type, the B-A transition is more or less blocked and the B-form steadily increases in proportion. Thus, the conformational flexibility of DNA is restricted in the anthraquinone complexes. Such an influence of a ligand on DNA is not rare and has been reported elsewhere [36,37,40]. The extent of anthracycline-induced inhibition is illustrated in fig. 2. Restriction of the conformational flexibility of DNA can even reach 100% and is found in the cases of ADM and DAM at relatively low values of  $r_i$ ; the  $r_i$  vs  $x_A$  plots of the drugs coincide with each other, as comprehended on the basis of their similarity in structure.

At somewhat higher values of  $r_i$ , ACM also blocks the B-A transition totally. In contrast, VBI appears to be unable to cause 100% inhibition of the conformational flexibility of DNA; a certain proportion of DNA (approx. 1/3) undergoes the B-A transition even at higher  $r_i$  values (0.1–0.2).

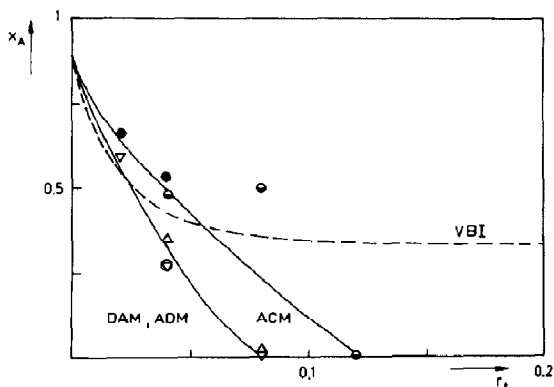


Fig. 2. Dependence of  $x_A$ , the fraction of A-DNA at medium relative humidity, on the binding ratio  $r_t$ , the number of anthraquinone molecules bound per DNA nucleotide. ( $\nabla$ ) Daunomycin; ( $\Delta$ ) adriamycin; ( $\bullet$ ,  $\circ$ ,  $\ominus$ ; different samples) aclinomycin A; for violamycin BI, symbols have been omitted for the sake of clarity.

The diverse effects of the various anthracycline antibiotics on DNA conformation as illustrated in fig. 2 may be interpreted as follows. A preference for B-form DNA as demonstrated by a decline in  $x_A$  can be considered to reflect drug intercalation, since this mechanism of binding is favoured in the case of B-DNA as shown previously for DAM [41–43]. Intercalation is well established as being the fundamental binding mechanism for the drugs studied [7,9,14,16,44–47]. The intercalated anthraquinone molecules apparently evoke long-range effects on conformational changes in DNA according to a recent report on other systems [37]; for instance, fixation of DNA in the B form by DAM and ADM at  $r_t = 0.08$  implies that the range of effect for a single drug molecule spans about six base-pairs on average, which correlates well with published data in the case of ADM [48]. This is a larger number than that immediately involved according to the neighbour-exclusion model. Long-range allosteric effects have also been reported for DAM with respect to DNA conformation [49].

ACM and, to an even greater extent, VBI are not as efficient as ADM and DAM at restricting the conformation of DNA to the B form. This may be interpreted in terms of the greater volume

of the sugar moieties of ACM and VBI being the probable cause of the lower degree of effectiveness as the dominant mode of binding for the case of intercalation than that occurring with ADM and DAM. Correspondingly, infrared LD and X-ray diffraction investigations performed in combination showed the fraction of externally bound drug at high  $r_t$  values to be greater for VBI than for DAM [17].

The presence of two sugar moieties in VBI bound at different positions on ring A was also taken as being indicative of the membrane permeability of this antibiotic in the case of peritoneal macrophages being much lower than for DAM [50]. Increasing values of the binding ratio in the DNA complexes not only lead to an absolute decline in  $x_A$ , but also simultaneously reduce the range of relative humidity for the A form. In other words, the boundary value for the limit to this range for the B-A transition shifts downwards from about 86% in pure DNA to 60% at lower  $x_A$  (e.g., at  $x_A < 0.5$ , the residual part of the A form is in most cases only detectable at R.H. < 75%, whereas in pure DNA, the fraction of A-form DNA is maximal at 75% R.H.).

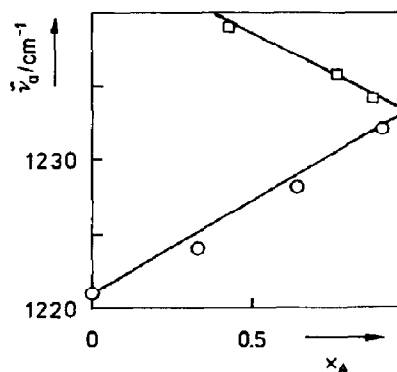


Fig. 3. Correlation between wave number of the band due to antisymmetric  $\text{PO}_2^-$  stretching vibration of DNA and the fraction of A-DNA in mixtures with B-DNA. (Lower plot) B-A transition; (upper plot) decline of A-DNA by disordering (different samples). Progression upwards along the curves signifies decreasing degree of hydration for the oriented DNA film being examined.

### 3.2. Drug binding to DNA phosphate detected spectroscopically

The reference values for pure DNA (at  $r_t = 0$ ) in table 1 provide confirmation of published data in showing that  $\bar{\nu}_a$  depends strongly on the relative humidity [19,20,22,51] and, consequently, on  $x_A$  (considering the B-A transition in fig. 3).

The latter dependence is linear, i.e.,  $\bar{\nu}_a$  is strictly correlated with the conformational pattern of DNA. On the basis of this linearity, it is possible to separate the contribution due to DNA confor-

mation from that arising via the introduction of drug to the effect on  $\bar{\nu}_a$ . It would be most instructive to compare the data at constant  $x_A$ . In the subsequent text, the case of high relative humidity is considered which corresponds to virtually pure B-DNA. By doing so, a significant decrease in  $\bar{\nu}_a$  becomes apparent on complexation for all the drugs investigated with the sole exception of DAM, a ligand practically without effect on the wave number.

It is reasonable to relate DAM firstly to the structurally analogous ADM. Their infrared spec-

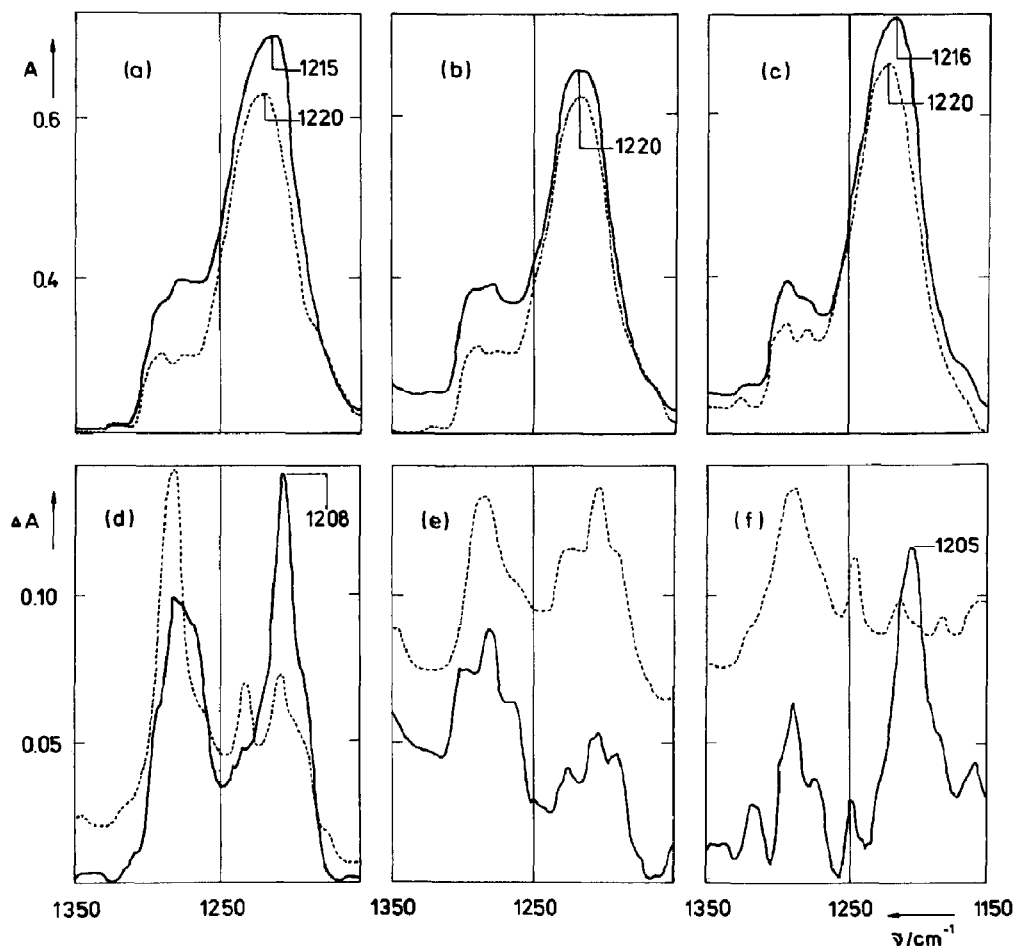


Fig. 4. Infrared spectra of DNA-adriamycin (a), DNA-daunomycin (b) and DNA-aclacinomycin A (c) complexes (—) together with the respective DNA spectra (.....) and difference spectra of DNA-bound ADM (d), DAM (e) and ACM (f) (—) compared to spectra of free drugs in KBr (-----). Spectra of DNA and of the complexes were obtained from oriented films at  $r_t = 0.08$  (ADM and DAM) and  $r_t = 0.04$  (ACM).

tra including the difference spectra of the DNA complexes are shown in fig. 4 (a, b, d and e). Since the structures of both drugs differ only in the presence of a surplus OH group at position 14 of ADM, the extra shift of  $5.5\text{ cm}^{-1}$  observed for ADM can be logically explained on the basis of an additional subsidiary hydrogen bond being formed between the C14-OH of intercalated ADM and the  $\text{PO}_2^-$  of DNA [18]. A corresponding C14-OH  $\cdots$   $\text{PO}_2^-$  interaction was also discussed very recently in the case of the association products formed by ADM and neutral phospholipids [52].

An infrared band near  $1070\text{ cm}^{-1}$  for ADM has been assigned in part to the C-O stretching vibration of the C14-OH group [53]. This assignment is confirmed on comparison of the infrared spectra of ADM and DAM (fig. 5): for ADM the absorption in the range  $1070\text{ cm}^{-1}$  is disproportionately stronger than for DAM when referred to other band intensities. On addition of DNA to ADM, drastic spectral changes occur in the  $1070\text{ cm}^{-1}$  band (see fig. 6): this band is split into two, i.e., at least one constituent undergoes a substantial shift in wave number. Provided that just the displaced component arises from C14-OH, this may then be taken as support for the above interpretation that the hydroxyl group in position C14 of ADM is hydrogen-bonded to a DNA phosphate.

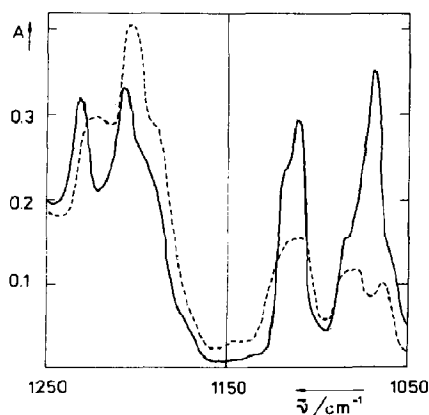


Fig. 5. Infrared spectra of adriamycin (—) and daunomycin (-----) obtained from KBr discs. The strongest absorption of ADM relative to DAM is found near  $1070\text{ cm}^{-1}$ .

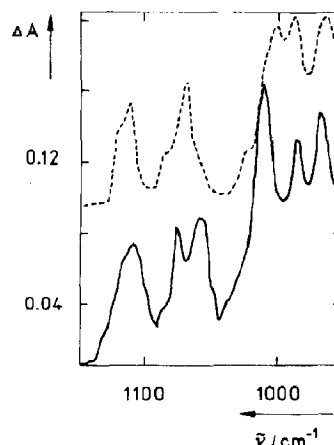


Fig. 6. Infrared spectra of DNA-bound adriamycin at  $r_1 = 0.08$  (—) and free ADM in KBr (-----).

Similarly, changes in the infrared bands assigned to OH deformations of trehalose were considered as an indication of hydrogen bonding occurring between carbohydrate and phospholipids in the sarcoplasmic reticulum [54].

The shape of the  $\nu_a$  band that is shifted somewhat due to the influence of anthraquinone drugs is also changed: before complexation, the band appears fairly symmetric (in the region of high relative humidity for B-DNA), however, following ligand addition, it becomes asymmetric with the absolute maximum lying more towards lower wave numbers (fig. 4a and c). This observation led us to generate the difference spectra for a number of DNA-bound drugs (see fig. 4d and f for ADM and ACM, respectively). This procedure yields 'new' bands with maxima at  $1208$  and  $1205\text{ cm}^{-1}$ , respectively. Comparison with the spectra for the free drugs indicates that the relative intensities are too high for one to be able to attribute them to the drugs alone. These bands are more appropriately explained as representing separated  $\nu_a$  difference bands indicating those particular  $\text{PO}_2^-$  groups which undergo specific interaction with suitable parts of or substituents on the anthraquinone derivatives. In the normal spectra, these bands are of course masked due to overlapping by those arising from non-interacting  $\text{PO}_2^-$  moieties; i.e., the observed shifts, amounting to only a few reciprocal



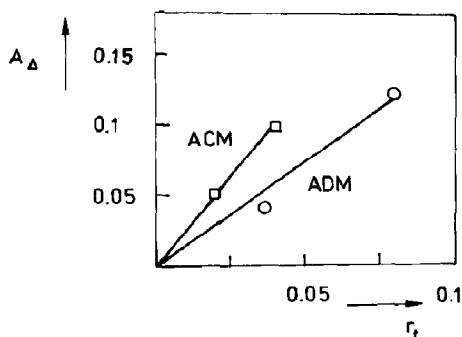


Fig. 7. Relationship between  $A_\Delta$ , the absorbance of the  $\text{PO}_2^-$  difference bands as shown in fig. 4d (adriamycin) and  $f$  (aclacinomycin A), and  $r_1$ , the drug binding ratio.

centimeters, do not reflect the real strength of the interaction. A better indication of this property is readily obtained on the basis of the degree of divergence between  $\nu_a$  of pure DNA and the position of the difference bands. In view of the magnitude of the shift in  $\bar{\nu}_a$  ( $12\text{--}15\text{ cm}^{-1}$ ) it is quite remarkable that any displacement in the normal spectra should be evident at all, if one takes into account that, at  $r_1 = 0.08$  for example, only about one in every 12  $\text{PO}_2^-$  groups can participate in subsidiary hydrogen bonding. The observation of a nonetheless significant shift in wave number for  $\text{PO}_2^-$  in the normal infrared spectra may arise from the fact that due to the hydrogen bonding interaction, a dramatic increase in the intensity of the  $\nu_a$  band also occurs, as discussed in a preceding paper [18]. Hence, the relatively small component arising from interacting  $\text{PO}_2^-$  groups makes a greater contribution to the total band than that from non-interacting  $\text{PO}_2^-$ .

Unfortunately, it was not possible to record reference spectra for the DNA-MX complex due to an irregular background. Thus, for MX as well as for VBI, only the decrease in  $\bar{\nu}_a$  that was observed for the ordinary infrared spectra was determined (see table 1).

With increasing values of  $r_1$  in the complexes, not only does the observed shift in  $\nu_a$  increase, as demonstrated by the data in table 1 for ADM, ACM, VBI and MX, but also the intensities of the  $\text{PO}_2^-$  difference bands due to ADM- and ACM-bound DNA. The plots in fig. 7 illustrate linear

behavior for each form of dependence. The influence on the  $\text{PO}_2^-$  groups of DNA is slightly stronger with ACM as compared to ADM, since for ACM (i) the slope of the linear plot in fig. 7 is somewhat greater; (ii) the wave number of the separated difference band is  $3\text{ cm}^{-1}$  lower.

At intermediate values of the relative humidity,  $\bar{\nu}_a$  of complexed DNA is determined, in each case, by the actual conformational flexibility, expressed by  $\chi_a$ , as well as by the further reduction in wave number evoked by the drug. For example, the fact that  $\bar{\nu}_a$  is independent of the relative humidity in the case of ADM at  $r_1 = 0.08$  demonstrates not only that DNA is completely frozen in the B conformation by bound drug molecules, but also that subsidiary hydrogen bonding of ADM to  $\text{PO}_2^-$  groups of DNA is maintained under conditions of intermediate relative humidity.

In the DNA-ADM system, the relevant drug substituent for the interaction with  $\text{PO}_2^-$  groups is almost obligatorily C14-OH. This interpretation is also in accordance with thermodynamic and kinetic data for the DNA-ADM and DNA-DAM complexes (cf. ref. 18). The question concerning the particular site involved in such  $\text{PO}_2^-$ -directed hydrogen bonding of ACM, VBI and MX is, however, more delicate. This binding site should satisfy both of the following prerequisites: (i) a comparable substituent must not be present on DAM; (ii) it must be located at the periphery of the molecular structure in order to be accessible to phosphate groups, i.e., substituents positioned on the central rings B and C of the chromophore cannot be accommodated to form hydrogen bonds between intercalated drug molecules and  $\text{PO}_2^-$  groups due to steric hindrance.

Regarding ACM and VBI first, the hydroxyl group at position C4 is the only one which fulfills both conditions listed above for these two compounds. However, compared to ADM, formation of the subsidiary hydrogen bond to DNA phosphate must be a more critical factor, since the C4-OH group in ACM and VBI is not as flexible and, consequently, not as adaptable as the C14-OH of ADM in the side-chain attached at position 9. Nevertheless, the C4-OH group is the most probable candidate for being involved in hydrogen-bond interaction with  $\text{PO}_2^-$  groups of DNA. Un-

fortunately, the related  $\nu(\text{C-O})$  band cannot be investigated in the same way as for ADM (cf. figs. 5 and 6), since it is located at about  $1210\text{ cm}^{-1}$  [53], i.e., where strong overlap occurs by the intense  $\nu_a$  band due to DNA. Accordingly, in NMR experiments on the complex formed between the self-complementary oligonucleotide duplex  $d(\text{CpCpTpApGpG})_2$  and ACM, a significant change was observed in the  $^1\text{H}$  chemical shift due to C4-OH, indicating the participation of this substituent in the interaction with DNA [55].

Concerning MX, all together there are four hydroxyl groups that satisfy the prerequisites for subsidiary  $\text{OH} \cdots \text{PO}_2^-$  hydrogen bonding: two at the side-chain termini and two at positions 1 and 4 of the ring systems. On the basis of their greater adaptability, we believe the side-chain hydroxyls to participate in hydrogen bonding with DNA phosphate rather than aromatic OH groups.

NMR analysis of  $d(\text{CpGpApTpCpG})_2$ -MX complexes revealed drastic variations in chemical shifts due to  $^{31}\text{P}$  resonances, thus demonstrating that phosphate groups may be involved in the binding of drug [56].

The formation of all of the hydrogen bonds proposed for anthraquinone binding to DNA phosphate necessitates exchange of previously bound water molecules with hydroxy substituents. The occurrence of such  $\text{C-OH} \cdots \text{PO}_2^-$  bonding was suggested in preceding studies of sugar binding to  $\text{PO}_2^-$  groups of DNA [57] and phospholipids [54].

### 3.3. Theoretical modeling of hydrogen-bonded drugs

In order to verify the validity of the hypothesis that phosphate vibrations are influenced by hydrogen-bonded anthraquinones, semi-empirical

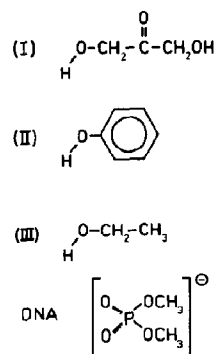


Fig. 8. Molecular fragments used in the theoretical CNDO/2 investigations to mimic DNA (bottom), adriamycin (I), alicinomycin A and violamycin B1 (II), and mitoxantrone (III).

quantum chemical calculations were performed on appropriate model fragments shown in fig. 8. In order to provide a spatial impression, the geometry of the phosphate-ADM fragment is illustrated in fig. 9. The results obtained on evaluation of the electronic and steric parameters by use of partial geometry optimization on the CNDO/2 level are summarised in table 2.

On forming a hydrogen bond, the covalent  $\text{P}=\text{O}$  bond strength, as indicated by the Wiberg bond index [58], is decreased to slightly differing extents. Simultaneously, closure of the  $\text{O}=\text{P}=\text{O}$  bond angle is evident. In both cases, the anthraquinones considered exert stronger effects than hydrogen-bonded water molecules.

With respect to different types of bonds, it has been known for several years that bond orders are correlated with stretching force constants [59–61]. These relationships are described as being predominantly linear in nature and can be used to

Table 2

Results of CNDO calculations on anthraquinone-phosphate interaction via hydrogen bonding (phosphate fragment and drug model notation, cf. fig. 8)

System	DNA	H <sub>2</sub> O-DNA	III-DNA MX-DNA	I-DNA ADM-DNA	II-DNA ACM-DNA
Wiberg bond index, $\text{WB}(\text{P}=\text{O})$	1.709	1.616	1.604	1.599	1.581
$\text{O}=\text{P}=\text{O}$ bond angle ( $^\circ$ )	116.1	114.8	114.6	114.5	114.2

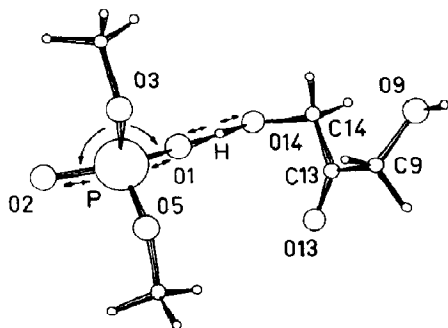


Fig. 9. Model of the hydrogen-bonding complex formed between a DNA fragment (fig. 8, bottom) and adriamycin (fig. 8, I). Arrows indicate unfrozen internal coordinates optimized during the calculations.

carry out normal coordinate analysis of the systems in question merely through treating the case of a DNA phosphate model  $\text{O}_2\text{P}(\text{OC})_2$  and varying the force constants and valence angles in order to mimic different ligands. The results of the normal coordinate analysis are presented in fig. 10. In the modeling, one  $\text{P}=\text{O}$  force constant is held at a fixed value while the other is varied according to the different hydrogen bond strengths. One observes from fig. 10 that the decreases in both  $\text{P}=\text{O}$  force constant and  $\text{O}=\text{P}=\text{O}$  bond angle evoke a corresponding change in the

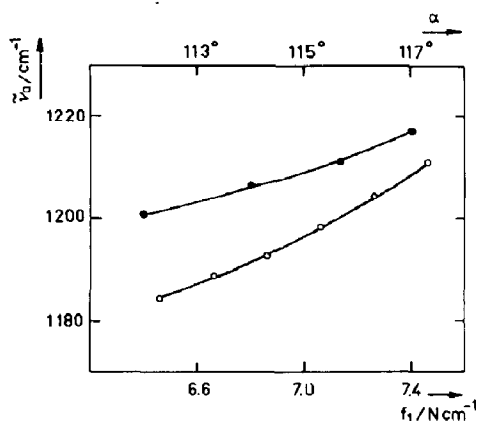


Fig. 10. Dependence of wave number of the antisymmetric vibration  $\tilde{\nu}_a$  on  $\text{P}=\text{O}$  force constant  $f_1$  ( $\circ$ — $\circ$ ) (at constant  $\alpha = 115.67^\circ$ ,  $f_2 = 7.459 \text{ N cm}^{-1}$ ), and on  $\text{O}=\text{P}=\text{O}$  bond angle  $\alpha$  ( $\bullet$ — $\bullet$ ) (at constant  $f_1 = f_2 = 7.459 \text{ N cm}^{-1}$ ) as calculated via normal coordinate analyses.

antisymmetric  $\text{PO}_2^-$  stretching vibration. Both effects give rise to a decrease in  $\tilde{\nu}_a$ , however, the major contribution to this process is that from the reduction in strength of the  $\text{P}=\text{O}$  bonds. If one assumes a 5% drop in the value of the force constant (7.459 to 7.059  $\text{N cm}^{-1}$ ), corresponding to the calculated change in Wiberg bond index, then the wave number will be shifted 13  $\text{cm}^{-1}$  (1211 to 1198  $\text{cm}^{-1}$ ) whereas further closure of the valence angle by  $1.7^\circ$  brings about an additional fall in wave number by 4  $\text{cm}^{-1}$ . Taking both effects into account, the hydrogen bonding of actual ligands should cause a total shift of 18–22  $\text{cm}^{-1}$ . These values transpired as being correct in both sign and order of magnitude on comparison with the decrease in  $\tilde{\nu}_a$  determined spectroscopically on the basis of the difference bands due to interacting  $\text{PO}_2^-$  groups (cf. fig. 4d and f).

The theoretical data in the two final columns of table 2 are in agreement with the infrared spectroscopic parameters discussed above (wave number of the difference bands; slopes of plots in fig. 7) in terms of ACM having a greater influence on the  $\tilde{\nu}_a$  band as compared to that of ADM.

In summary, comparative semi-empirical molecular orbital calculations in combination with normal coordinate analysis confirm the infrared data in two respects: (i) the concept of hydrogen bonding of anthraquinone substituents to terminal phosphate-oxygen atoms; and (ii) the stronger hydrogen-bonding affinity of anthraquinones to  $\text{PO}_2^-$  moieties (correlated with a larger shift in  $\tilde{\nu}_a$ ) in comparison with water.

It should be noted that, for phospholipids, OH groups (due to the sugar trehalose) also induce a somewhat greater extent of reduction of  $\tilde{\nu}_a$  than water [54]. This is interpreted in terms of stabilization of phospholipid-trehalose association by hydrogen bonding under conditions for dehydration [54].

### 3.4. Model considerations on DNA-anthraquinone complexes

The geometrical models of the DNA-anthraquinone interaction established thus far refer mostly to the DNA-DAM complex and, as de-

rived therefrom, the DNA-ADM complex. In the previous paper [18], it could be stated that the idea of subsidiary hydrogen bonding of ADM via C14-OH to DNA phosphate is, in principle, compatible with the models of both Pigram et al. [7] and Quigley et al. [9], but not with that proposed by Henry [8]. The DNA-DAM model derived from fiber X-ray diffraction analysis by Pigram et al. predicts an electrostatic interaction and hydrogen bonding of the  $\text{NH}_3^+$  group of daunosamine to the  $\text{PO}_2^-$  moiety of DNA in the major groove [7]. The extension of this model to ADM as performed by Neidle [62], demonstrates that such a mechanism of sugar binding in no way conflicts with the subsidiary hydrogen bond proposed in ref. 18, since the locus of the electrostatic interaction is two residues away from the intercalation site. On the other hand, in the model of Quigley et al., based on X-ray diffraction analysis of a crystalline complex between the self-complementary duplex  $\text{d}(\text{CpGpTpApCpG})_2$  and DAM [9], confirmed through considerations of local mobility [63], the amino sugar is positioned in the minor groove of DNA and does not undergo binding. The infrared spectral data of the current study do not allow unequivocal conclusions to be drawn as regards the sugar moiety being located in the minor or major groove of DNA. Furthermore, the existence of an  $\text{NH}_3^+ \cdots \text{PO}_2^-$  interaction could not be demonstrated, since this would also have been required to become evident from the DNA-DAM system, for which no additional shift in  $\tilde{\nu}_a$  was observed. Most probably, electrostatic interactions involving  $\text{PO}_2^-$  groups are suppressed by the extremely high ionic strength of the strongly condensed films of polyionic DNA with added salt. Moreover, it can be suggested that, for ADM, e.g.,

this screening effect prevents the formation of a feasible hydrogen bond,  $\text{N}^+-\text{H} \cdots \text{O}^-$ , since the electrostatic term for hydrogen bonds with charged donor and acceptor atoms is very large. The disadvantages of a (drug) ammonium-to-(DNA)phosphate interaction may also extend to the C4'-OH groups adjacent to  $\text{NH}_3^+$  of the amino sugar. Therefore, C4'-OH does not participate in a  $\text{PO}_2^-$ -directed hydrogen bond although this should be possible from a theoretical viewpoint with a probability comparable to that for other terminal hydroxyl groups of the drugs actually involved (see section 3.3).

Based on the models for the hexanucleotide-DAM complex, two possible modes of participation by the C14-OH group of ADM in DNA binding were additionally discussed: in the preliminary paper [9], direct hydrogen bonding between the drug C14-OH group and the O3' atom of DNA phosphate involved in a C-O-P ester bond was postulated; very recently, the alternate C14-OH interaction with the  $\text{PO}_2^-$  moiety via a water bridge has been proposed on the grounds of further refined single-crystal X-ray diffraction analysis [64,65]. The relevance of both hydrogen-bonding systems has been assessed through further quantum-chemical calculations. The results are listed in table 3. In the case where ADM is bound to O1 of DNA phosphate by a water linkage, the data are very similar to those for attachment by pure water. The attack on the O3' oxygen by ADM was calculated to yield an even weaker effect than water binding to O1. Thus, both of the mechanisms proposed by Wang et al. [9,64] do not provide a satisfactory explanation for the actually observed  $\tilde{\nu}_a$  shift being larger than for water molecules.

Table 3

Quantum-chemical results for adriamycin-phosphate interaction by different types of hydrogen bonds including mechanisms proposed in the literature [9,65]

Hydrogen bond geometry	DNA (without hydrogen bond)	$\text{H}_2\text{O}$ - O1(DNA)	ADM(C14-OH) – DNA(phosphate)		
			ADM-O3' [9]	ADM-H <sub>2</sub> O-O1 [65]	ADM-O1 (table 1)
Wiberg bond index, $\text{WB}(\text{P}=\text{O})$	1.709	1.616	1.717	1.615	1.599
$\text{O}=\text{P}=\text{O}$ bond angle (°)	116.1	114.8	115.7	114.8	114.5

The concepts employed in the models of DNA-ACM and DNA-MX intercalation are at present not as detailed as for the DNA-DAM and DNA-ADM systems. An approximate model concerning the hexanucleotide-ACM complex mentioned above [55] was presented which has the C4-OH group of ACM in close contact with the phosphate group linking the thymidine and adenosine residues in the central part of the oligonucleotide (see fig. 7 in ref. 55). This model is closely compatible with our proposal for the hydrogen bond formed between the C4-OH groups of ACM and VBI and  $\text{PO}_2^-$  groups of DNA.

Regarding the DNA-MX intercalation complexes, modeling via computer graphics predicts the MX side chains to be located in the major groove of DNA [56]. One can readily imagine that they can be accommodated, being attached at  $\text{PO}_2^-$  groups by hydrogen bonds via their terminal OH groups. Theoretical considerations suggest the involvement of the phosphate O1 atom in the binding for MX side chains [66].

#### 4. Conclusions

Investigation of DNA complexes employing infrared spectroscopy strongly suggests that some anthraquinone anticancer drugs are able to form hydrogen bonds to the  $\text{PO}_2^-$  groups of the DNA backbone. Such hydrogen bonds are almost unique to the anthraquinones and are undetectable for a large number of other ligands (cf. refs. 36 and 40). Subsidiary hydrogen bonding has only been observed where the following prerequisites of the system had been fulfilled: (i) the drug must have a fundamental mode of binding to DNA of intercalation; (ii) the substituents involved in hydrogen bonds must be sterically accessible to the  $\text{PO}_2^-$  groups; i.e., they must be located at the periphery of the drug molecule; (iii) the affinity for hydrogen bonding or hydrogen donor strength of the anthraquinone substituents must be greater than that of water, which is present in the samples in excess; (iv) the substituents must not bear charges. All of these preconditions are satisfied by a number of different selected hydroxyl groups of the anthraquinones adriamycin, aclacinomycin A,

violamycin BI and mitoxantrone in the intercalated state.

Subsidiary hydrogen bonding by these OH groups to the  $\text{PO}_2^-$  moieties of DNA can be considered as stabilizing the overall binding of drug to DNA and, possibly, as enhancing the antitumor activity of the drugs which is exerted by interference with the functioning of DNA. Thus, the attachment of suitable hydroxyl substituents to the drug chromophores may be important in further efforts at development in drug design. Since hydrogen bonding of this type has also been observed in interactions between phospholipids and drugs or carbohydrates, it is tempting to suggest that  $\text{C-OH} \cdots \text{PO}_2^-$  hydrogen bonds are of general importance in biological systems.

#### Acknowledgements

The authors are indebted to Drs. H. Berg, H. Fritzsche and G. Löber for critical reading of the manuscript and to Mrs. M. Richter and Mrs. M. Teichmann for skilful technical assistance. The anthraquinone samples were generous gifts from Dr. Arcamone (daunomycin and adriamycin), Dr. Umezawa (aclacinomycin A), Dr. Schwabe (mitoxantrone) and Mr. Koch (violamycin BI).

#### References

- 1 F. Arcamone, in: *Topics in antibiotic chemistry*, Vol. 2, ed. P.G. Sammes (Wiley, Chichester, 1978) p. 102.
- 2 T. Oki, Y. Matsuzawa, A. Yoshimoto, K. Numata, I. Kitamura, S. Hori, A. Takamatsu, H. Umezawa, M. Ishizuka, H. Naganawa, H. Suda, M. Hamada and T. Takeuchi, *J. Antibiot.* 28 (1975) 830.
- 3 T. Oki, *J. Antibiot.* 30, suppl. (1977) 70.
- 4 R.K.-Y. Zee-Cheng and C.C. Cheng, *J. Med. Chem.* 21 (1978) 291.
- 5 K.C. Murdock, R.G. Child, P.F. Fabio and R.B. Angier, *J. Med. Chem.* 22 (1979) 1024.
- 6 S.T. Crooke and S.D. Reich, *Anthracyclines: current status and new developments* (Academic Press, New York, 1980).
- 7 W.J. Pigram, W. Fuller and L.D. Hamilton, *Nature New Biol.* 235 (1972) 17.
- 8 D.W. Henry, *Am. Chem. Soc., Symp. Ser.* 30 (1976) 15.
- 9 G.J. Quigley, A.H.-J. Wang, G. Ughetto, G. van der Marel, J.H. van Boom and A. Rich, *Proc. Natl. Acad. Sci. U.S.A.* 77 (1980) 7204.

- 10 M. Manfait, A.J.P. Alix, P. Jeannesson, J.-C. Jardillier and T. Theophanides, *Nucleic Acids Res.* 10 (1982) 3803.
- 11 F. Quadrioglio, A. Ciana, G. Manzini, A. Zaccara and F. Zunino, *Int. J. Biol. Macromol.* 4 (1982) 413.
- 12 H. Berg, H. Fritzsche, W. Ihn, P. Mühlig, W. Pohle, K.-E. Reinert, H. Schütz, E. Stutter, D. Tresselt, H. Triebel, A. Walter and K. Weller, *Sitzungsber. Sächs. Akad. Wiss. Leipzig, Math.-Naturwiss. Klasse* 120 (1988) 1.
- 13 W. Pohle, *Stud. Biophys.*, submitted for publications.
- 14 W. Fleck, D.G. Strauss, W. Koch, P. Kramer and H. Prauser, D.D.R. – Patentschrift 100494 (*Int. Cl.*: 12d, 9/14).
- 15 G. Löber, R. Klarner, E. Smekal, T. Räm, Z. Balcarova, J. Koudelka and V. Kleinwachter, *Int. J. Biochem.* 15 (1983) 663.
- 16 T. Räm and W. Pohle, *Mol. Biol.* 20 (1986) 1313.
- 17 W. Pohle and T. Räm, *Biomed. Biochim. Acta* 48 (1989) 377.
- 18 W. Pohle and J. Flemming, *J. Biomol. Struct. Dyn.* 4 (1986) 243.
- 19 T. Shimanouchi, M. Tsuboi and Y. Kyogoku, *Adv. Chem. Phys.* 7 (1964) 435.
- 20 W. Pohle and M. Bohl, *Stud. Biophys.* 122 (1987) 113.
- 21 R.E. Franklin and R.G. Gosling, *Acta Crystallogr.* 6 (1953) 673.
- 22 J. Pilet and J. Brahms, *Biopolymers* 12 (1973) 387.
- 23 W. Pohle, V.B. Zhurkin and H. Fritzsche, *Biopolymers* 23 (1984) 2603.
- 24 J. Pitha, *Biochim. Biophys. Acta* 232 (1971) 607.
- 25 R.D.B. Fraser, *J. Chem. Phys.* 21 (1953) 1511.
- 26 W. Pohle and H. Fritzsche, *Stud. Biophys.* 82 (1981) 81.
- 27 J.A. Pople and D.L. Beveridge, *Approximate molecular orbital theory* (McGraw-Hill, New York, 1970).
- 28 P. Scharfenberg, *Computer program CNDO/CNDOO5*, Institut für Wirkstoffforschung, Berlin (1974).
- 29 S. Arnott, S.D. Dover and A.J. Wonacott, *Acta Crystallogr. B* 25 (1969) 2192.
- 30 R.B. von Dreele and J.J. Einck, *Acta Crystallogr. B* 33 (1977) 3283.
- 31 R.N. Jones, *Computer programs for infrared spectrophotometry – Normal coordinate analysis – N.R.C.C. Bulletin no. 15*, Canada (1976).
- 32 D.F. McIntosh and K.H. Michaelian, *Can. J. Spectrosc.* 24 (1979) 35, 65.
- 33 K.C. Lu, E.W. Prohofsky and L.L. van Zandt, *Biopolymers* 16 (1977) 2491.
- 34 J. Flemming, W. Pohle and M. Richter, *Stud. Biophys.* 104 (1984) 97.
- 35 R.E. Dickerson, H.R. Drew, B.N. Conner, R.M. Wing, A.V. Fratini and M.L. Kopka, *Science* 216 (1982) 475.
- 36 W. Pohle and H. Fritzsche, *Stud. Biophys.* 104 (1984) 303.
- 37 H. Fritzsche, A. Rupprecht and M. Richter, *Nucleic Acids Res.* 12 (1984) 9165.
- 38 R.M. Wartell and J.T. Harrell, *Biochemistry* 25 (1986) 2664.
- 39 R. Brandes, R.R. Vold, D.R. Kearns and A. Rupprecht, *Biopolymers* 27 (1988) 1159.
- 40 W. Pohle, H. Fritzsche and M. Richter, *Stud. Biophys.* 81 (1980) 127.
- 41 J. Doskocil and I. Fric, *FEBS Lett.* 37 (1973) 55.
- 42 T.W. Plumbbridge and J.R. Brown, *Biochim. Biophys. Acta* 479 (1977) 441.
- 43 J.B. Chaires, *Nucleic Acids Res.* 11 (1983) 8485.
- 44 W. Kersten, H. Kersten and E. Szybalski, *Biochemistry* 5 (1966) 236.
- 45 F. Zunino, A. Gambetta, A. DiMarco and A. Zaccara, *Biochim. Biophys. Acta* 277 (1972) 489.
- 46 J. Kapuscinski, Z. Darzynkiewicz, F. Traganos and M.R. Melamed, *Biochem. Pharmacol.* 30 (1981) 231.
- 47 J.W. Lown, C.C. Hanstock, R.D. Bradley and D. Scraba, *Mol. Pharmacol.* 25 (1984) 178.
- 48 P.D. van Helden, *Nucleic Acids Res.* 11 (1983) 8415.
- 49 J.B. Chaires, *Biochemistry* 24 (1985) 7479.
- 50 K. Augsten and D.G. Strauss, *Stud. Biophys.* 104 (1984) 219.
- 51 E. Taillandier, J. Liquier and J.A. Taboury, in: *Advances in infrared and Raman spectroscopy*, eds. R.J. Clark and R.E. Hester (Wiley, New York, 1985) vol. 12, p. 65.
- 52 A.M. Giuliani, C.A. Boicelli, L. de Angelis, M. Giomini, M. Giustini and E. Trotta, *Stud. Biophys.* 123 (1988) 45.
- 53 E. Goormaghtigh and J.M. Ruyschaert, *Res. Commun. Chem. Pathol. Pharmacol.* 42 (1983) 149.
- 54 J.H. Crowe, L.M. Crowe and D. Chapman, *Arch. Biochem. Biophys.* 232 (1984) 400.
- 55 S. Takahashi, N. Nagashima, Y. Nishimura and M. Tsuboi, *Chem. Pharm. Bull.* 34 (1986) 4494.
- 56 G. Kotovych, J.W. Lown and J.P.K. Tong, *J. Biomol. Struct. Dyn.* 4 (1986) 111.
- 57 S.J. Webb and M.D. Dumasia, *Can. J. Microbiol.* 14 (1968) 841.
- 58 K.B. Wiberg, *Tetrahedron* 24 (1968) 1083.
- 59 R.J. Gillespie and E.A. Robinson, *Can. J. Chem.* 41 (1963) 2074.
- 60 E.A. Robinson and M.W. Lister, *Can. J. Chem.* 41 (1963) 2988.
- 61 A.C. Chapman, D.A. Long and D.T.L. Jones, *Spectrochim. Acta* 21 (1965) 633.
- 62 S. Neidle, *Cancer Treatm. Rep.* 61 (1977) 928.
- 63 S.R. Holbrook, A.H.-J. Wang, A. Rich and S.-H. Kim, *J. Mol. Biol.* 199 (1988) 349.
- 64 A.H.-J. Wang, G. Ughetto, G.J. Quigley and A. Rich, *Biochemistry* 26 (1987) 1152.
- 65 A.H.-J. Wang, in: *Nucleic acids and molecular biology*, vol. 1, eds. F. Eckstein and D.M.J. Lilley (Springer, Berlin, 1987) p. 53.
- 66 K.-X. Chen, N. Gresh and B. Pullman, *Nucleic Acids Res.* 14 (1986) 3799.